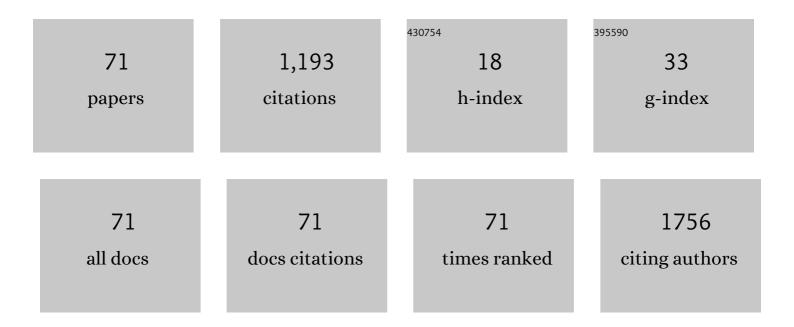
List of Publications by Year in descending order

Source: https://exaly.com/author-pdf/6009649/publications.pdf Version: 2024-02-01



#	Article	IF	CITATIONS
1	Nucleation and dissociation of carbon dioxide hydrate in the inter- and intra-particle pores of dioctahedral smectite: Mechanistic insights from molecular dynamics simulations. Applied Clay Science, 2022, 216, 106344.	2.6	16
2	sp ² -to-sp ³ transitions in graphite during cold-compression. Physical Chemistry Chemical Physics, 2022, 24, 10561-10566.	1.3	2
3	Insights into Carbon Dioxide Hydrate Nucleation on the External Basal Surface of Clay Minerals from Molecular Dynamics Simulations. ACS Sustainable Chemistry and Engineering, 2022, 10, 6358-6369.	3.2	14
4	Quasi-elastic neutron scattering (QENS) and its application for investigating the hydration of cement-based materials: State-of-the-art. Materials Characterization, 2021, 172, 110890.	1.9	14
5	Influences of thermal damage on water transport in heat-treated cement mortar: Experimental and theoretical analyses. Construction and Building Materials, 2021, 288, 123100.	3.2	22
6	Antiperovskite Ionic Conductor Layer for Stabilizing the Interface of NASICON Solid Electrolyte Against Li Metal in Allâ€Solidâ€State Batteries**. Batteries and Supercaps, 2021, 4, 1491-1498.	2.4	23
7	High-Pressure and High-Temperature Synthesis and In Situ High-Pressure Synchrotron X-ray Diffraction Study of HfSi ₂ . Inorganic Chemistry, 2021, 60, 15215-15222.	1.9	3
8	Layered Co/Ni-free Mn-rich oxide P2-Na2/3Mn0.8Fe0.1Mg0.1O2 as high-performance cathode material for sodium-ion batteries. Ionics, 2020, 26, 735-743.	1.2	22
9	Local Structural Changes and Inductive Effects on Ion Conduction in Antiperovskite Solid Electrolytes. Chemistry of Materials, 2020, 32, 8827-8835.	3.2	19
10	Al Substitution Induced Differences in Materials Structure and Electrochemical Performance of Ni-Rich Layered Cathodes for Lithium-Ion Batteries. Journal of Physical Chemistry C, 2019, 123, 19298-19306.	1.5	25
11	Application of In-beam Activation Analysis in Elemental Distribution Analysis. IOP Conference Series: Materials Science and Engineering, 2019, 563, 022050.	0.3	0
12	Water sorptivity of unsaturated fractured sandstone: Fractal modeling and neutron radiography experiment. Advances in Water Resources, 2019, 130, 172-183.	1.7	20
13	Application of neutron imaging to investigate fundamental aspects of durability of cement-based materials: A review. Cement and Concrete Research, 2018, 108, 152-166.	4.6	136
14	Characterization of unsaturated diffusivity of tight sandstones using neutron radiography. International Journal of Heat and Mass Transfer, 2018, 124, 693-705.	2.5	19
15	Improving the Performance of Layered Oxide Cathode Materials with Footballâ€Like Hierarchical Structure for Naâ€lon Batteries by Incorporating Mg ²⁺ into Vacancies in Naâ€lon Layers. ChemSusChem, 2018, 11, 1223-1231.	3.6	35
16	A solvent â€~squeezing' strategy to graft ethylenediamine on Cu3(BTC)2 for highly efficient CO2/CO separation. Chemical Engineering Science, 2018, 184, 85-92.	1.9	31
17	3D neutron tomography of steel reinforcement corrosion in cement-based composites. Construction and Building Materials, 2018, 162, 561-565.	3.2	28
18	Modulating the Electrochemical Performances of Layered Cathode Materials for Sodium Ion Batteries through Tuning Coulombic Repulsion between Negatively Charged TMO ₂ Slabs. ACS Applied Materials & Interfaces, 2018, 10, 1707-1718.	4.0	34

#	Article	IF	CITATIONS
19	Simulations and systematic neutron beam characterisations on two-dimensional position-sensitive neutron detector multi-wire proportional counter with delay-line readout. Journal of Instrumentation, 2018, 13, T08012-T08012.	0.5	0
20	Visualization of rapid penetration of water into cracked cement mortar using neutron radiography. Materials Letters, 2017, 195, 1-4.	1.3	20
21	A Study on Inhomogeneous Neutron Intensity Distribution Origin from Neutron Guide Transportation. Physics Procedia, 2017, 88, 354-360.	1.2	2
22	Decreasing Li/Ni Disorder and Improving the Electrochemical Performances of Ni-Rich LiNi _{0.8} Co _{0.1} Mn _{0.1} O ₂ by Ca Doping. Inorganic Chemistry, 2017, 56, 8355-8362.	1.9	171
23	Effects of microstructure on water imbibition in sandstones using Xâ€ray computed tomography and neutron radiography. Journal of Geophysical Research: Solid Earth, 2017, 122, 4963-4981.	1.4	39
24	Ultrastrong Boron Frameworks in ZrB ₁₂ : A Highway for Electron Conducting. Advanced Materials, 2017, 29, 1604003.	11.1	71
25	Facile Synthesis and Enhanced Electrochemical Performances of Hierarchical ZnFe2O4-Graphene Hybrid as an Anode Material for Li-Ion Batteries. Journal of Nanoscience and Nanotechnology, 2017, 17, 2093-2097.	0.9	0
26	Structural and multiferroic properties of Pr and Ti co-doped BiFeO 3 ceramics. Ceramics International, 2016, 42, 14675-14678.	2.3	8
27	A charged metal–organic framework for CO2/CH4 and CO2/N2 separation. Inorganica Chimica Acta, 2016, 443, 299-303.	1.2	16
28	Neutron diffraction analysis and electrochemical performance of spinel Ni(Mn2â^'Co)O4 as anode materials for lithium ion battery. Materials Research Bulletin, 2016, 77, 265-270.	2.7	10
29	Ultrahigh cycling stability and rate capability of ZnFe ₂ O ₄ @graphene hybrid anode prepared through a facile syn-graphenization strategy. New Journal of Chemistry, 2016, 40, 3139-3146.	1.4	15
30	Characterization of a Real-time Neutron Imaging Test Station at China Advanced Research Reactor. Physics Procedia, 2015, 69, 79-86.	1.2	2
31	Hardness, elastic, and electronic properties of chromium monoboride. Applied Physics Letters, 2015, 106, .	1.5	54
32	Fe3O4@porous carbon hybrid as the anode material for a lithium-ion battery: performance optimization by composition and microstructure tailoring. New Journal of Chemistry, 2015, 39, 3435-3443.	1.4	17
33	The synergic effects of Na and K co-doping on the crystal structure and electrochemical properties of Li4Ti5O12 as anode material for lithium ion battery. Solid State Sciences, 2015, 44, 39-44.	1.5	49
34	A study on optical aberrations in parabolic neutron guides. Nuclear Instruments and Methods in Physics Research, Section A: Accelerators, Spectrometers, Detectors and Associated Equipment, 2015, 786, 17-22.	0.7	1
35	Experience of the Indirect Neutron Radiography Method Based on the X-ray Imaging Plate at CARR. Physics Procedia, 2015, 69, 258-264.	1.2	7
36	Simulation of Fast Neutron Radiography with a Time-of-Flight System. Physics Procedia, 2015, 69, 284-291.	1.2	0

#	Article	IF	CITATIONS
37	The effects of Co doping on the crystal structure and electrochemical performance of Mg(Mn2Ââ^'ÂxCox)O4 negative materials for lithium ion battery. Solid State Sciences, 2015, 39, 23-28.	1.5	15
38	Large-scale scientific facility at China Advanced Research Reactor for neutron scattering. Chinese Science Bulletin, 2015, 60, 2068-2078.	0.4	3
39	Influence of Y and Al co-doping on the crystal structure and magnetic properties of Nd2â^'xYxFe17â^'yAly. Intermetallics, 2014, 55, 199-203.	1.8	2
40	Structural and thermodynamic characteristics of sH 2,2-dimethylbutane-methane deuterohydrate. Journal of Chemical Thermodynamics, 2014, 77, 82-86.	1.0	2
41	Design of the Testing Set-up for a Nuclear Fuel Rod by Neutron Radiography at CARR. Physics Procedia, 2013, 43, 307-313.	1.2	6
42	New Type of Neutron Image Scintillator based on H310BO3/ZnS(Ag). Physics Procedia, 2013, 43, 216-222.	1.2	2
43	Improving the Electrochemical Performance of Li ₄ Ti ₅ O ₁₂ Anode through Confinement into Ordered Bimodal Porous Carbon Frameworks. Journal of Physical Chemistry C, 2013, 117, 26889-26895.	1.5	16
44	X-ray analysis on crystal structures of crystalline polyimides. , 2013, , .		0
45	Design of Real-time Neutron Radiography at China Advanced Research Reactor. Physics Procedia, 2013, 43, 48-53.	1.2	14
46	Design of Cold Neutron Imaging Facility at China Advanced Research Reactor. Physics Procedia, 2013, 43, 73-78.	1.2	14
47	Study of glycol chitosan-carboxymethyl β-cyclodextrins as anticancer drugs carrier. Carbohydrate Polymers, 2013, 93, 679-685.	5.1	25
48	Crystal structure of tetraaqua-bis(4-(1,2,4-triazol-4-yl)benzoato-κN)-zinc(II) decahydrate, C18H40N6O18Zn. Zeitschrift Fur Kristallographie - New Crystal Structures, 2013, 228, 319-320.	0.1	0
49	Crystallographic Studies of Nd _{3-x} Y _x Fe _{27.5} TM _{1.5} (0.6â‰æâ‰û.4, TM=Ti, Mo) Compounds. Advanced Materials Research, 2013, 785-786, 634-637.	0.3	0
50	Crystal structure of catena-[μ2-bis(biphenyl-2,2'-dicarboxylato-O:O')]- (μ2-pyrazine-N:N')dicobalt(II), Co(C4H4N2)(C14H8O4)2. Zeitschrift Fur Kristallographie - New Crystal Structures, 2012, 227, .	0.1	0
51	Phase transition and negative thermal expansion properties of Sc2â^'xCrxMo3O12. Ceramics International, 2012, 38, 6525-6529.	2.3	21
52	Crystal structure and negative thermal expansion of solid solution Y2W3â^'xMoxO12. Journal of Materials Science, 2011, 46, 5160-5164.	1.7	7
53	Crystal structure and negative thermal expansion of solid solution Lu2W3â^'x Mo x O12. International Journal of Minerals, Metallurgy and Materials, 2010, 17, 786-790.	2.4	8
54	Crystal structure and negative thermal expansion of solid solution Yb ₂ W _{3-x} Mo _x O ₁₂ . Materials at High Temperatures, 2010, 27, 151-156.	0.5	4

#	Article	IF	CITATIONS
55	A Porous Metalâ^'Organic Replica of α-PbO ₂ for Capture of Nerve Agent Surrogate. Journal of the American Chemical Society, 2010, 132, 17996-17999.	6.6	66
56	Neutron powder diffraction study and B-site ordering in microwave dielectric ceramics Ba(Ca1/3Nb2/3)O3. Solid State Sciences, 2009, 11, 170-175.	1.5	7
57	Crystal structure and negative thermal expansion properties of solid solution Er2W3â^'xMoxO12. Transactions of Nonferrous Metals Society of China, 2009, 19, 1623-1627.	1.7	7
58	Structure and magnetic properties of Nd3â^'xDyxFe23â^'yCo6Moy (x=0.5–3) compounds. Solid State Sciences, 2008, 10, 1412-1415.	1.5	1
59	Formation, structure and magnetic properties of Nd3â^'xZrxFe27.8Mo1.2 (0.1â‰æâ‰0.5) compounds. Journal of Alloys and Compounds, 2007, 431, 68-71.	2.8	2
60	Crystallographic structure and magnetic properties of NdyDy1â^'yFe11â^'xTiCox compounds. Journal of Alloys and Compounds, 2007, 438, 21-24.	2.8	2
61	Investigations on the structural and magnetic properties of doubly substituted Nd2Fe17â^'xâ^'yTixGay compounds (0≤â‰≇.0, 0â‰ÿâ‰≇). Journal of Alloys and Compounds, 2006, 407, 58-64.	2.8	2
62	Crystallographic and magnetic properties of (Nd,Dy)3Fe27.5(Ti,Mo)1.5 compounds. Journal of Magnetism and Magnetic Materials, 2006, 301, 415-421.	1.0	2
63	Effects of the substitution of Al for Fe on phase transition, crystal structures, and magnetic properties of Nd3(Fe,Ti)29-type intermetallics. Journal of Applied Physics, 2006, 100, 103910.	1.1	1
64	Cooperative effects of a combined substitution on the magnetic properties of Nd2â^'xYxFe17â^'ySiy intermetallic compounds (0⩽x⩽1.5,0⩽y⩽3.0). Journal of Applied Physics, 2006, 99, 023904.	1.1	4
65	Effects of substitution of Dy for Nd on the structural and magnetic properties of Nd3ⰒxDyxFe27.5Mo1.5 (0.3⩽x⩽1.8). Physica B: Condensed Matter, 2005, 367, 275-281.	1.3	1
66	Structure and magnetic properties of (Nd,Y)3(Fe,Co,Ti)29 compounds. Physica B: Condensed Matter, 2005, 369, 266-272.	1.3	3
67	The effect of Zr addition on the formation and structural properties of 3:29 compounds in the Fe–Nd–Ti–Zr system. Journal of Physics Condensed Matter, 2005, 17, 6007-6014.	0.7	2
68	Effects of double substitution on the magnetic properties of Nd2Fe17â^'xâ^'yTixAly: A combined investigation of x-ray diffraction, neutron diffraction, and magnetic measurement. Journal of Applied Physics, 2005, 98, 013537.	1.1	3
69	Structure analysis of Nd3â^'xYxFe23â^'yCo6Moy (x=0.36–3.0;y=1.1,0.9) compounds. Journal of Applied Physics, 2005, 98, 033903.	1.1	0
70	The effects of the combined substitution of Y and Ga on the crystallographic structure of Nd2â^'xYxFe17â^'yGay intermetallic compounds. Journal of Alloys and Compounds, 2005, 400, 178-183.	2.8	2
71	Synthesis and structural properties of Nd3â^'xYxFe27.5Ti0.8Mo0.4(0⩽x⩽1.8) and Nd3â^'x′Yx′Fe27 intermetallic compounds. Journal of Alloys and Compounds, 2005, 403, 168-175.	.8Mg1.2(0) <x′⩽ 4</x′⩽